HHS Public Access

Author manuscript

Mol Psychiatry. Author manuscript; available in PMC 2016 December 21.

Published in final edited form as:

Mol Psychiatry. 2017 January ; 22(1): 56–67. doi:10.1038/mp.2016.17.

Persistent inhibitory circuit defects and disrupted social behavior following *in utero* exogenous cannabinoid exposure

Geoffrey A. Vargish[1], **Kenneth A. Pelkey**[1], **Xiaoqing Yuan**[1], **Ramesh Chittajallu**[1], **David Collins**[1], **Calvin Fang**[1], and **Chris J. McBain**[1]

[1]Program in Developmental Neurobiology, *Eunice Kennedy-Shriver* National Institute of Child Health and Human Development, National Institutes of Health, Bethesda, Maryland 20892

Abstract

Placental transfer of Δ9-tetrahydrocannabinol (THC) during pregnancy has the potential to interfere with endogenous cannabinoid regulation of fetal nervous system development *in utero*. Here we examined the effect of maternal cannabinoid intake on mouse hippocampal interneurons largely focusing on cholecystokinin containing interneurons (CCK-INTs), a prominent cannabinoid subtype 1 receptor (CB1R) expressing neuronal population throughout development. Maternal treatment with THC or the synthetic CB1R agonist WIN55,212-2 (WIN) produced a significant loss of CCK-INTs in offspring. Further, residual CCK-INTs in animals prenatally treated with WIN displayed decreased dendritic complexity. Consistent with these anatomical deficits, pups born to cannabinoid treated dams exhibited compromised CCK-INT mediated feedforward and feedback inhibition. Moreover, pups exposed to WIN *in utero* lacked constitutive CB1R mediated suppression of inhibition from residual CCK-INTs, and displayed altered social behavior. Our findings add to a growing list of potential cell/circuit underpinnings that may underlie cognitive impairments in offspring of mothers that abuse marijuana during pregnancy.

Introduction

Marijuana is one of the most widely abused illicit drugs amongst pregnant women [1], and the ever increasing social and legal acceptance of recreational cannabis use is likely to escalate consumption within this cohort. As THC, the major psychoactive ingredient in marijuana, efficiently undergoes cross placental transfer, maternal cannabis use has the potential to interfere with ongoing fetal development *in utero*[2]. Given the rise in THC content of recreationally available cannabis strains and the increasing prevalence of potent cannabis-based waxes/oils, even moderate consumption during pregnancy may be sufficient to disrupt embryonic development[3, 4]. While regulatory obstacles have limited research on prenatal cannabis exposure, a handful of studies in both human subjects and animal models have established that prenatal and perinatal cannabis exposure promotes various cognitive,

Correspondence to: Chris J. McBain, mcbainc@mail.nih.gov.

Conflict of Interest Statement:
The authors have no conflicts of interest.

behavioral, and neuropsychiatric defects, indicating that embryonic nervous system patterning is particularly susceptible to maternal cannabis abuse [5–9]. However, the cellular and molecular mechanisms underlying prenatal THC induced changes in neuronal circuitry remain poorly understood.

In the brain, THC acts at the cannabinoid family of receptors, where it can disrupt cellular communication mediated by the endogenous cannabinoids 2-arachidonyl glycerol or anandamide[10]. During nervous system development endocannabinoid (eCB) signaling, primarily through cannabinoid subtype 1 receptors (CB1Rs), has been implicated in neuronal proliferation, migration, morphogenesis and synaptogenesis [11–13]. In particular, a number of studies have implicated CB1R signaling as critical for proper axon pathfinding and connectivity of developing neocortical glutamatergic long-range projection neurons[13–18]. During embryonic development CB1Rs are also strongly expressed by caudal ganglionic eminence- (CGE-) derived GABAergic interneurons and in the mature brain, hippocampal cholecystokinin-expressing interneurons (CCK-INTs) are the dominant CB1R expressing neuronal population [11, 12, 19–22]. The long tangential migration necessary for CGE-derived interneurons to reach the hippocampus combined with the known influence of eCB signaling on CCK-INT growth cone dynamics, migration and morphogenesis suggests that these cells may be particularly vulnerable to maternal cannabinoid intake[11, 12, 22]. Thus, we examined how chronic prenatal exposure to exogenous cannabinoids influences postnatal CCK-INT patterning and function using combined immunohistochemistry, electrophysiology, and behavioral analyses.

We found that prenatal exposure to exogenous cannabinoids significantly reduces the density of CCK-INTs and similarly reduces the density of CCK axon terminals in CA1 stratum pyramidal. These anatomical deficits translate to a reduction in CCK-INT mediated spontaneous synaptic inhibition as well as CCK-INT mediated feedforward and feedback inhibition in the CA1 microcircuit. Further, we demonstrate a loss of constitutive CB1R activity in residual CCK-INTs, and concomitant deficits in social interactions of mice following prenatal exogenous cannabinoid treatment. These findings add to a growing list of cellular and network deficits that may underlie neurobehavioral deficits observed in individuals exposed to exogenous cannabinoids *in utero* following maternal cannabis use.

Materials and Methods

Animals

All experiments were conducted in accordance with animal protocols approved by NIH. All experiments were performed on *5HT3AR*-GFP or *Nkx2.1-cre:RCE-GFP* reporter lines as indicated. Timed pregnancy was performed by breeding male transgenics with either WT C57/BL6 or transgenic females. The date of plug was noted as embryonic day 0.5 (E0.5). Pregnant females were then given daily intraperitoneal injections with THC (5 mg/kg, suspended in 5% ethanol+5% corn oil in saline), or WIN55,212-2 (0.75 mg/kg, suspended in 0.3% Tween 80 in saline) from E10.5–E18.5. Experiments were then performed on the offspring age p14–p45 as indicated. Exogenous cannabinoid (THC or WIN) treated females were always run in parallel with a corresponding vehicle (VH) treated mouse so that each THC or WIN litter could be assayed in parallel with an appropriate VH control litter.

Females used for injection were only used once to minimize potential for cross-generational effects of cannabinoid administration.

Immunohistochemistry

For immunohistochemical analyses, mice were perfused transcardially using 4% paraformaldehyde/1xPBS solution. Brains were removed and postfixed overnight at 4°C followed by cryoprotection using 25% sucrose/1xPBS solution. 50 μm horizontal sections were cut on a freezing microtome and washed in 1XPBS. For parvalbumin (PV), somatostatin (SOM), calretinin (CR), vasoactive intestinal peptide (VIP), cannabinoid subtype 1 receptor (CB1R) and embryonic GFP labeling brain slices were permeabilized and blocked in 1xPBS+1%BSA+10% normal goat serum+0.5% Triton X-100 (Carrier PB) at room temperature for 2 hours followed by incubation in primary antibodies diluted with 1XPBS+1%BSA+1% normal goat serum+ 0.1%Triton X-100 (Carrier Solution; mouse anti-PV (Sigma P3088) 1:3000, rabbit anti-SOM (DAKO A0566) 1:1000, rabbit anti-CR (Millipore/Chemicon AB5054) 1:1000, guinea pig anti VIP (Pennisula Laboratories, T-5030) 1:1000, rabbit anti-CB1R (Cayman 10006590) 1:1000) 1:2500, chicken anti-GFP (Aves Labs Inc. 0511FP12) overnight at 4°C. After thorough washing in Carrier Solution, brain slices were incubated with secondary antibodies (Alexa Fluor 555 conjugated goat anti-mouse IgG, Alexa Fluor 555 conjugated goat anti-rabbit IgG, Life Technologies) diluted in Carrier Solution (1:1000) at room temperature for 1–2 hours. Following another thorough wash in 1xPBS, sections were mounted on gelatin-coated slides Prolong Gold (Life Technologies).

For embryonic immunohistochemistry, mouse embryos were removed at E16.5 and heads were drop fixed in 4% paraformaldehyde/1xPBS solution overnight at 4° C. Brains were then removed and cryoprotected using a 25% sucrose/1xPBS solution. Brains were then embedded in optimal cutting temperature compound (OCT) and frozen at −80° C. 18 μm coronal sections were cut using a cryostat and slide mounted. Labeling for CB1R and GFP in embryonic tissue was performed as described above.

For cholecystokinin (CCK) staining, brain slices were treated with 3% H_2O_2/1xPBS at room temperature for 30 minutes before permeabilization and blockage. After incubation with mouse anti-CCK (CURE, 1:1000) at 4°C for 48 hours, slices were incubated with biotinylated goat anti-mouse IgG (Vector Laboratories, 1:200) for 2 hours at room temperature. Mouse ABC Elite kit (Vector Laboratories) was used for detection in combination with tetramethylrhodamine conjugated tyramide (TSA System, Perkin Elmer) to amplify and visualize the signal.

For cell counting fluorescent images were captured using an Olympus AX-70 fluorescent microscope with a Retiga 4000R cooled CCD camera (Qimaging, Surrey, Canada). At least 3 independent pairs from three separate litters of VH control and THC or WIN treated mice were used at P20–P30 for quantitative analysis. For each interneuron marker, 10x images of hippocampi from 4 non-adjacent sections from each mouse were used to count in the CA1-CA3 area. For GFP+ cell counts we focused on the granule cell-hilar border of the dentate gyrus, an area enriched with CCK-INTs[23], as the promiscuity of CCK immunoreactivity in this region precludes analysis of CCK-INT density (eg. see Fig 1A).

For analysis of CB1R labeling high resolution single confocal images were taken using a 63x water immersion objective on a Zeiss LSM 510 microscope. Counting was performed on four hippocampal sections from each animal. Quantitative analysis of CB1R-positive puncta density in the CA1 pyramidal cell layer was performed using ImageJ. Watershed parameters that best approximated manual puncta determination were established for each set of VH and exogenous cannabinoid treated mice and applied universally to all sections in that set. Images were converted to binary using ImageJ's automated "Make Binary" function.

Electrophysiology

Hippocampal slices (300 μm thick) were prepared from P14–P45 WIN or VH treated mice as indicated. Animals were anesthetized with isoflurane and the brain was dissected in ice-cold saline solution (in mM): 130 NaCl, 24 $NaHCO_3$, 10mM glucose 3.5 KCl, 1.25 mM NaH_2PO_4, 1 $CaCl_2$ and 5 $MgCl_2$, saturated with 95% O_2 and 5% CO_2, pH 7.4. Horizontal hippocampal slices were cut using a VT-1000S vibratome (Leica Microsystems, Bannockburn, IL) and incubated in saline solution at 35° C until recording. Slices were transferred to a submerged recording chamber and perfused (3–5 mL/min, 32–35° C) with artificial cerebrospinal fluid (ACSF; in mM): 130 NaCl, 24 $NaHCO_3$, 10mM glucose 3.5 KCl, 1.25 mM NaH_2PO_4, 2.5 $CaCl_2$ and 1.5 $MgCl_2$ saturated with 95% oxygen and 5% CO_2, pH 7.4. For feedforward inhibition experiments $CaCl_2$ was increased to 4.5mM to enhance the efficacy of synaptic transmission and recordings were done in the presence of the $GABA_B$ receptor antagonist CGP55845 (1μM). 50–100μM dl-AP5 and 10μM DNQX was applied to ACSF to isolate spontaneous inhibitory postsynaptic currents (sIPSCs) during recordings of spontaneous activity as well as IPSCs during monosynaptically evoked experiments and 10μM bicuculline was used to confirm the inhibitory nature of the responses. Spontaneous excitatory postsynaptic currents (sEPSCs) were pharmacologically isolated with 10μM bicuculline. In addition, 250nM AgTx, 1μM WIN55,212-2, 10μM CCh and 10μM AM251 were used as specified. CA1 pyramidal cells were visually identified using IR-DIC video microscopy (Hamamatsu Orca-ER) and were targeted for whole-cell recording using a computer-controlled multiclamp 700A amplifier (Axon Instruments, Foster City, CA). Putative CCK-INTs were identified in *5HT3AR-GFP* mice by GFP expression excited by a Lambda SC light source (Sutter Instruments) and visualized online via video fluorescence microscopy (Hamamatsu Orca-ER). Recording electrodes (5–7 MΩ) were pulled from borosilicate glass (WPI, Sarasota, FL) and filled with one of three intracellular solutions (in mM): 1) 130 CsCl, 8.5 NaCl, 5 HEPES, 4 $MgCl_2$, 4 Na_2ATP, 0.3 NaGTP and 1 QX-314 (Tocris), pH 7.2–7.3, 290 mOsm for sEPSC, sIPSC, eIPSC and uIPSC recordings; 2) 130 K-gluconate, 0.6 EGTA, 10 HEPES, 2 $MgCl_2$, 2 Na_2ATP, 0.3 NaGTP and 6 KCl, pH 7.2–7.3, 290 mOsm for presynaptic CCK-INTs in paired recordings; 3) 137 $CsCH_3SO_4$, 4.5 NaCl, 10 HEPES, 4 MgATP, 0.3 NaGTP, 1 QX-314, pH 7.2–7.3, 290 mOsm for feedforward inhibition experiments. 0.2% biocytin was added for recordings of CCK-INTs for *post hoc* morphological processing of recorded cells to confirm basket cell or Schaffer-collateral associated cell anatomy using fluorescently conjugated avidin. A subset of pyramidal cells were also biocytin recovered for anatomical evaluation where indicated. Uncompensated series resistance, 5–15 MΩ, was monitored and recordings were discarded if changes of >10% occurred. sIPSCs/sEPSCs were detected and analyzed in Clampfit using a

template-based detection method from 30s of gap-free recording. Recordings of sEPSCs, sIPSCs, eIPSCs and uIPSCs were performed at a holding potential of −70mV. For each cell, all detected events were averaged to create a representative sIPSC or sEPSC waveform, which was used for analysis of amplitude. For DSI of sIPSCs slices were treated with CCh to enhance the CCK-INT mediated portion of sIPSC inhibitory drive[24]. sIPSC DSI was evoked by applying a voltage step from −70mV to 0mV for a duration of 5s approximately 1 min after onset of CCh evoked activity. Amplitude, frequency and charge (area under the curve) were measured in 5s bins preceding and following the depolarization. DSI was calculated by expressing amplitude, frequency and charge following the depolarization as a percentage of baseline values obtained prior to the 5s depolarization. Synaptic stimulation was applied via a constant current isolation unit (A360, WPI) connected to a patch electrode filled with oxygenated ACSF. Synaptic events for disynaptic feedback inhibition and monosynaptic basket cell inhibition experiments were evoked by low intensity stimulation (200μs/10–80μA) in the alveus and CA1 pyramidal cell layer, respectively. During feedback inhibition experiments CA1 pyramidal cell population spikes were monitored with a field recording electrode filled with ACSF placed in stratum pyramidale. Disynaptic feedforward inhibition was evaluated in the Schaffer collateral to CA1 pyramidal cell pathway by placing the stimulating electrode in CA1 stratum radiatum in slices with a cut made between CA3 and CA1 to prevent recurrent excitation of the CA3 network. To eliminate any potential confounding monosynaptic IPSC contamination of feedforward inhibitory waveforms, events obtained in the presence of DNQX were digitally subtracted from baseline feedforward inhibitory waveforms. Only recordings with monsynaptic IPSC contamination of less than 50% were included for analysis. For paired recordings, presynaptic interneuron action potentials were evoked by a 2ms current step of 2nA from −70mV while holding the postsynaptic PC at −70mV in voltage clamp. 25 pulse trains at 50 Hz were delivered every 10s for analysis of asynchronous release. To determine asynchronicity, the area under the curve was measured from a 300ms window centered on the peak of the last AP in the evoked train. The area under the curve of a 150ms window immediately preceding the train was then subtracted to account for the contribution of sIPSCs. Three trials were measured and averaged to determine the amount of asynchronous release for each cell. For DSI, two 2ms current steps at 50Hz were delivered presynaptically every 10s. The postsynaptic cell was depolarized for 2s to 0mV before every fourth trial. DSI was calculated as the percent change in amplitude of 10 IPSCs recorded immediately preceding depolarization and 10 IPSCs recorded after the depolarization. All data were acquired at a sampling rate of 10kHz using Pclamp10.2 (Molecular Devices) and filtered at 3kHz.

Unitary analysis was performed for paired recordings. For each cell a minimum of 20 trials was analyzed. Potency was determined as the amplitude of the postsynaptic response without failures while unitary amplitude included failures. For paired pulse ratio a pair of presynaptic action potentials was delivered at 50Hz and the amplitude of the second postsynaptic response was divided by the amplitude of the first postsynaptic response. Latency was measured as the time from the peak of the presynaptic action potential to the beginning of the postsynaptic response. Jitter was then measured as the standard deviation of the latency across 20 or more trials for each cell.

Cell Morphology

Slices containing biocytin filled cells were drop fixed in 4% paraformaldehyde overnight at 4°C then permeabilized and incubated with Alexa-555 conjugated avidin (Molecular Probes). Following multiple washes slices were resectioned (70 μm) on a freezing microtome (Microm) and mounted on gelatin coated slides using Mowiol (Calbiochem) mounting medium. Stacked Z-section images of recorded cells revealed by biocytin conjugation were obtained with a Leica TCS SP2 RS confocal microscope. Semi-automated 3D reconstruction was performed for each cell using the Simple Neurite Tracer plugin for ImageJ. Sholl analysis for each cell was performed on compressed image stacks of the reconstructed cells in ImageJ. Terminal density was determined by counting the number of boutons along a randomly selected continuous ~100 μm section of axon in single optical sections. Boutons were visually identified as enlarged varicosities/puncta along the parent axon[25]. Precise length of the sampled axon segment was determined using Simple Neurite Tracer. The number of boutons was then normalized to the measured axon length for each cell.

Behavioral Analyses

For behavioral testing we used adult *5HT3A-GFP* males treated prenatally with either WIN55,212-2 or vehicle. All animals were 8–12 weeks old at the time of testing. All tests were done during the light phase. Social interaction was tested using a three chamber apparatus as previously described[26]. The apparatus was made of clear plexiglass with each chamber measuring 20cm × 40.5cm × 22cm and with openings of 10cm × 5cm in the dividing walls allowing free access. Three 10-minute trials were performed in succession for each mouse. For the first 10 minutes the mouse was confined to the center of the apparatus and allowed to habituate. For the second 10-minute trial, the doors were removed for the outside chambers and the mouse was allowed to freely explore the entire apparatus. For the third trial, a wire pencil holder was placed in one side chamber representing the novel object and a wire pencil holder with a non-littermate WT C57/BL6 male was placed in the other side chamber. Mice were then allowed to freely explore the arena. Entries into the chambers as well as distance and immobility measurements were analyzed using ANY-maze (Stoelting Co., Wood Dale, IL). Interaction time was measured manually by a blinded observer with interaction being defined as sniffing of either the wire cup or wire cup with the mouse. The mouse was considered to be sniffing when the subject's nose was directed at the wire cup and the distance between the nose and the cup was less than ~2cm. Anxiety-like behavior was measured using the elevated plus maze (San Diego Instruments, San Diego, CA), which consisted of an elevated platform in the shape of an equilateral cross (Height: 38.75, Platform width: 5cm, Arm length: 30.5cm), with two opposing arms protected by walls (Height: 15.25cm). The mice were initially placed in the center of the apparatus facing the closed arms and were allowed to free explore the apparatus for 10 minutes. Any mice that fell off the apparatus (n=1) were immediately returned to the apparatus at the approximate location of the fall and the behavior was noted. Each session was video recorded and analyzed using ANY-maze software (Stoelting Co., Wood Dale, IL).

Real-time RT-PCR

Hippocampi from P30 VH and WIN treated mice were isolated. Total RNA was prepared using an RNAqueos-4PCR kit (ThermoFisher Scientific). cDNA was generated using a High Capacity RNA-to-cDNA kit (Applied Biosystems). Yield was estimated using both spectrophotometry as single strand DNA and agarose gel electrophoresis in comparison to DNA standards. Quantitative PCR was carried out using a StepOne instrument from Applied Biosystems. Comparative C_T experiments were designed and setup using Design Wizard software (Applied Biosystems). cDNAs from VH and WIN hippocampi were used at 50 ng for each 20 μl reaction. Daglalpha and Magl were targeted using FAM-Daglalpha (Mm00813830-m1, Applied Biosystems) and FAM-Mgll (Mm00449274-m1, Applied Biosystems) respectively. VIC-Gapdh (Mm9999915, Applied Biosystems) was used as an endogenous control. Real-time PCR was run under the thermal profile: 50°C, 2 min; 95°C, 10 min; 40 cycles of 95°C, 15 s; 60°C, 1 min. 4 independent real-time PCR experiments were performed using RNA prepared from independent mouse brains from independent litters. In each PCR, 3 replicates were run for each sample/target. PCR analysis was performed using the StepOne software (Applied Biosystems). Cycle threshold (C_T) for each targeted gene was determined relative to the C_T of the endogenous control gene gapdh to obtain ΔC_T values. The relative abundance of a targeted gene within the sample in relation to gapdh was then calculated as $2^{\Delta CT}$.

Statistics

Statistical analyses were carried out in OriginPro (Origin Lab, MA). All data was tested for normality using Shapiro Wilk normality test and then tested for significance using either a Student's t-test or Mann-Whitney U test as appropriate. All values represent mean±SEM.

Results

Reduced CCK-INT density and altered CCK-INT morphology following in utero exogenous cannabinoid exposure

Previous in depth embryonic characterization revealed the caudal ganglionic eminence (CGE) as the primary source of CB1R expressing interneurons (INTs) with unexpectedly high levels of CB1R expression observed in CGE-derived migrating interneurons, beginning at embryonic day 12.5 (E12.5), that infiltrate the developing hippocampus as early as E13.5 and continuing through birth[20] (and see Suppl Fig 1). Thus, to focus our study on interneurons, we modeled chronic recreational prenatal cannabis use with daily intraperitoneal injections of exogenous cannabinoids (primarily WIN [0.75 mg/kg], but also THC [5mg/kg] in a subset of experiments) in pregnant mice from E10.5 until birth and compared the offspring with those from vehicle (VH) treated controls. Exogenous cannabinoid doses were chosen to mimic moderate cannabis use without disrupting pregnancy success rates[27, 28]. Indeed prenatal injections did not adversely affect pregnancy outcomes as there were no differences between VH and WIN treated mothers in the rate of weight gain during pregnancy, litter size, and pup weight gain postnatally (Suppl Fig 2). Following prenatal injections, we examined the density of select hippocampal INT populations in pups aged P20–P30 when interneuron densities have reached mature levels and specific interneuron markers are sufficiently expressed for immunohistochemistry[29, 30].

The density of CCK-INTs was consistently and significantly reduced following prenatal exposure to THC or WIN compared to VH controls assayed in parallel (Fig 1A–C). This effect was specific to CCK-INTs as there was no significant difference observed for parvalbumin, (PV), somatostatin, (SOM), calretinin (CR) or vasoactive intestinal peptide (VIP) expressing INT densities (Fig 1A–C), consistent with strong localization of CB1Rs to CCK-INTs but not the other subpopulations assayed.

To verify whether the CCK-INT reduction results from cell loss or reduced immunoreactivity of CCK-8, we examined GFP expression in *5HT3AR-GFP* mice that comprehensively label CGE-derived INTs, including CCK-INTs. We focused on the dentate granule cell-hilar border, an area known to be enriched in CCK-INTs[19] but where CCK immunolabeling within mossy fibers precludes analysis of CCK-INTs using immunohistochemistry in the mouse (e.g. see Fig 1A). For comparison we also examined *NKX2.1-cre:RCE-GFP* mice that label medial ganglionic eminence derived INTs, including PV+ and SOM+ populations [31, 32]. GFP+ cell density was significantly reduced in *5HT3AR-GFP* mice, but not *NKX2.1-cre:RCE-GFP* mice following prenatal WIN treatment (Fig 1D). In fact, GFP+ cell density was significantly reduced throughout the entire hippocampus of *5HT3A-GFP* mice following *in utero* WIN exposure, with deficits emerging as early as P10. (Supp Fig 3). Thus, with regards to effects on hippocampal interneurons, chronic prenatal exogenous cannabinoid exposure promotes selective loss of CGE-derived CCK-INTs. It is worth noting that though CCK-INTs were the only population examined to reliably exhibit a deficit, other interneuron subpopulations trended towards being reduced as well. Modest changes in the CGE-derived VIP+ population may reflect the limited overlap of this population with CCK-BCs[33, 34] and a minor cohort of immature CGE-derived CR+ INTs express CB1Rs[20]. These observations combined with our reliable CCK-INT deficit could reflect a cell autonomous effect of prenatal WIN treatment on CB1R expressing interneuron cohorts. However, the weak trends for reduced PV and SOM immunoreactive INTs following WIN treatment would be difficult to reconcile with a cell autonomous effect on CB1R expressing populations. Indeed though SOM and CCK transcripts have been found in single developing INTs[11] and one report has suggested functional CB1R expression in mature neocortical SOM-INTs[35], PV and SOM MGE-derived INT cohorts are not generally recognized to express CB1Rs. As we did not observe significant changes in the overall *NKX2.1-cre:RCE-GFP* population, the modest changes in PV and SOM immunoreactivities could be secondary to altered network driven changes in the expression of these activity regulated proteins[36].

Consistent with the loss of CCK-INTs, WIN treated mice exhibited a significant reduction in the density of CB1R+ boutons in stratum pyramidale (SP), the major axon termination zone of perisomatic targeting CCK cells (Fig 1E). A previous study suggested that prenatal exogenous cannabinoid treatment disrupts CB1R+ terminal basket formation in the cortex due to impaired axon targeting[15]. However, morphological evaluation of 5-HT3AR-GFP+ basket (BC) and Schaffer collateral associated (SCA) cells, two major subtypes of CCK-INTs[37], revealed comparable axon trajectories and bouton densities between WIN and VH treated mice (Fig 1F–G). Thus, the decrease in CB1R+ terminals innervating SP in WIN treated mice primarily reflects reduced absolute CCK-INT numbers rather than gross defects in residual CCK-INT axonal patterning. Further evaluation revealed decreased dendritic

complexity of both CCK-BCs and SCAs in WIN treated animals as well as decreased overall dendritic length in CCK-BCs (Fig 1F, H–I). These dendritic alterations are consistent with eCB regulation of neurite development in culture[11], and could impair circuit recruitment of remaining CCK-INTs.

CB1Rs are also present on forebrain glutamatergic principal neurons and developmental disruption of eCB signaling in these cells impairs long-range corticofugal and corticospinal axon projections [14, 15, 17, 18, 38]. Thus, we examined if our CCK-INT deficit in prenatally WIN treated pups was accompanied by changes within the hippocampal pyramidal cell (PC) population. Analysis of PC densities in the CA1 hippocampal region of P20–30 mice did not reveal any differences between VH and WIN treated animals (Fig 2B). In addition, prenatal WIN exposure did not produce any obvious defects in axonal projections within the fimbria and corpus callosum (Fig 2A). Morphological analysis of individual cells also showed that dendritic length of CA1 PCs was comparable in VH and WIN treated mice (Fig 2C). Moreover, maternal WIN treatment did not alter basic excitatory synaptic properties of hippocampal PCs as CA1 sEPSCs and Schaffer-collateral evoked synaptic input-output relations were similar in pups from VH and WIN treated groups (Fig 2D–E). Taken together, these findings indicate that prenatal WIN exposure affects CGE-derived CCK-INTs without overt disruption of hippocampal PCs.

Prenatal exogenous cannabinoid treatment reduces CCK-INT mediated spontaneous, feedforward, and feedback inhibition

To assess the impact of prenatal WIN exposure on inhibitory function we electrophysiologically assayed CA1 PC spontaneous inhibitory postsynaptic currents (sIPSCs) in age matched (P14–P25) VH and WIN treated mice. Initially, we found no difference in the amplitude or frequency of pharmacologically isolated sIPSCs recorded from animals treated with WIN or VH (Suppl Fig 4). While these findings appear inconsistent with a loss of CCK-INTs, sIPSCs capture events mediated by various INT subtypes. To specifically assay CCK-INT mediated spontaneous inhibition, we probed the extent of depolarization-induced suppression of inhibition (DSI). DSI reflects an eCB mediated retrograde signal that inhibits GABA release from presynaptic CCK-INTs and can be evoked by depolarizing recorded PCs to promote eCB production and release [39, 40]. Cells recorded from animals prenatally treated with WIN exhibited significantly less DSI compared to VH controls (Fig 3A). Importantly, in paired recordings between individual remaining CCK-INTs and PCs DSI remained intact in WIN treated mice (see below, Fig 4) indicating that the reduction in DSI sensitive spontaneous inhibition likely results from reduced CCK-INTs rather than altered eCB signaling.

To further probe CCK-INT driven inhibitory tone we assayed feedback inhibition in the CA1 microcircuit in age matched (P30–P45) VH and WIN treated mice[41]. While recording from CA1 PCs we stimulated the alveus to evoke back-propagating action potentials in PC axons that disynaptically recruits inhibition from a heterogeneous population of CA1 INTs (Fig 3B). Acute application of WIN revealed a deficient CCK-INT mediated component to feedback inhibition in WIN treated animals (Fig 3C). Normalizing the degree of CCK-INT mediated feedback inhibition to overall CA1 PC excitation, measured by simultaneously

monitored CA1 population spikes (PSs), confirmed a significant disruption in the balance between CCK-INT driven feedback inhibition and CA1 PC population activity in WIN treated mice (IPSC/PS ratios in WIN treated mice were 36.4±11.5% of those in VH treated mice, VH: n=16 cells/11 animals/6 litters WIN: n=14 cells/9 animals/7 litters, p=0.04). Because the altered dendritic morphology of CCK-INTs in WIN treated mice could alter synaptic recruitment and different interneuron subtypes provide distinct temporal contributions to feedback inhibition [41], we also examined trains of disynaptic IPSCs to increase the opportunity for CCK-INT recruitment. However, prenatally WIN treated mice continued to exhibit less acute WIN sensitivity of disynaptic IPSCs throughout the train (Fig 3E).

Recent evidence suggests that CCK-INTs also significantly contribute to feedforward inhibition in the hippocampal CA3 to CA1 pathway [42]. To assess feedforward inhibition, we recorded from CA1 PCs while stimulating Schaffer collaterals in CA1 stratum radiatum (Fig 3F). For these experiments the chloride reversal potential was set to −80 mV and CA1 PCs were held at −30 mV so that disynaptic inhibitory components could be easily separated from monosynaptic excitatory events. Consistent with the observed loss in CCK-INTs, WIN treated mice exhibited reduced DSI sensitivity of feedforward inhibition (Fig 3F). Thus, prenatal exogenous cannabinoid exposure significantly alters circuit inhibition dynamics in a manner consistent with CCK-INT loss.

In utero exogenous cannabinoid exposure reduces constitutive CB1R activity but preserves other basic synaptic properties of residual CCK INTs

Constitutive CB1R activation inhibits transmitter release from CCK-BCs. Thus, CB1R antagonism increases CCK-BC release probability yielding a larger IPSC [43], and the degree of this basal CB1R activity scales with ongoing circuit activity [44]. To examine if the reduction in CCK-INTs following prenatal WIN exposure homeostatically changes constitutive CB1R inhibition of residual CCK-BC output, we recorded CA1 PCs while stimulating SP to evoke monosynaptic IPSCs from CCK-BCs in slices from age matched (p14–P25) VH and WIN treated mice (Fig 4A). Slices were incubated with ω-agatoxin IVa (250nM) to prevent PV-BC output[45], and the remaining CCK-BC driven IPSC was probed for constitutive CB1R activity. The CB1R antagonist AM251 increased the amplitude of monosynaptically evoked IPSCs for both single events and trains of events in VH treated animals (Fig 4A–B). However, this effect was absent in animals prenatally exposed to WIN revealing a loss of constitutive CB1R activation in residual CCK-BCs (Fig 4A–B). While reduced constitutive CB1R activity following *in utero* WIN exposure may serve to maximize the function of remaining CCK-INTs during basic circuit activity, more complex computations requiring activity dependent scaling of CCK-BC synapses could suffer.

To further examine the synaptic properties of residual CCK-INTs in mice treated prenatally with WIN, we recorded connected CCK-BC and SCA to PC pairs in slices from age matched (P14–P25) VH and WIN treated mice (Fig 4C). Both CCK-BCs and SCAs had similar potency, unitary amplitude, release probability, latency and jitter between VH and WIN treated animals (Suppl Fig 5). Despite the lack of constitutive CB1R activity in WIN treated CCK-BCs, we observed similar DSI levels between VH and WIN treated mice

confirming normal CB1R function at remaining CCK-INT to PC connections (Fig 4C). This also confirms that activity driven eCB signaling in PCs remains intact following *in utero* WIN treatment, consistent with RT qPCR data showing no difference in the relative abundance of the eCB synthesizing [diacylglycerol lipase α (DAGLα)] or hydrolyzing [monoacylglycerol lipase (MAGL)] enzymes, in VH and WIN treated mice (Suppl Fig 6). CCK-INTs in both VH and WIN treated animals also exhibited prominent asynchronous release during high frequency activity, a hallmark feature of CCK-INT transmission (Fig 4D). Thus, the basic synaptic properties of remaining CCK-INTs are largely preserved following prenatal exogenous cannabinoid exposure.

Deficits in social interaction following prenatal exogenous cannabinoid exposure

Finally, we investigated potential behavioral consequences of CCK-INT deficits in WIN treated animals. While there is currently no evidence linking CCK-INT dysfunction to particular behavioral phenotypes, autism associated neuroligin-3 mutants exhibit reduced constitutive CB1R activity at CCK-INT to PC synapses similar to our findings in WIN treated mice [46]. Moreover, perinatal exogenous cannabinoid treatment reduces social interaction in rats[47]. Thus, we used the three-chamber social interaction test to assay social behavior (Fig 5A). We found no difference between WIN and VH treatment groups in the number of entries made into the chamber containing either the novel mouse or object (Fig 5B). However, WIN treated mice spent significantly less time interacting with the novel mouse compared to VH controls, indicating a deficit in social interaction (Fig 5C). This deficit is not an indirect effect of increased anxiety, since on the elevated plus maze we found no difference between WIN and VH treated animals in the number of entries/time spent in the open or closed arms or the number of head dips (Fig 5D–F). These findings indicate that prenatal exposure to exogenous cannabinoids results in specific deficits in social interaction. Though our findings of disrupted CCK-INT function and altered social behavior are only correlational, a potential mechanistic link would be consistent with similar social deficits in the neuroligin-3 mutant model, which also lacks constitutive CB1R activity.

Discussion

The effect of prenatal and perinatal exposure to exogenous cannabinoids on behavioral outcomes has been well documented in animal models and humans. However, little is known about the effect of prenatal cannabinoid exposure at cellular and molecular levels. In this study, we present evidence that prenatal exposure to exogenous cannabinoids impacts the development of hippocampal CCK-INTs. Our data indicate that *in utero* exposure to CB1R agonists significantly reduces the density of CCK-INTs and, similarly, reduces CB1R+ bouton density in CA1 stratum pyramidal. These anatomical deficits result in a significant decrease in CCK-INT mediated spontaneous inhibition as well as deficits in CCK-INT mediated feedforward/feedback inhibition in the CA1 microcircuit. Further, prenatal exposure to WIN significantly reduced dendritic complexity as well as overall dendritic length, and reduced constitutive CB1R activity in residual CCK-INTs. Finally, we show that prenatal WIN exposure produces deficits in social interaction, suggesting CCK-INT loss may contribute to the generation of persistent neurobehavioral deficits observed in individuals prenatally exposed to cannabis.

Two recent studies have examined the impact of prenatal exposure to exogenous cannabinoids on cortical circuitry and neuronal migration, respectively [15, 22]. In the former, Tortoriello et al. (2014) show that repeated Δ9-THC exposure during midgestation modulates SCG10/stathmin-2 availability, ultimately inducing alterations to cytoskeletal elements in fetal neurons. This results in disruption of cortical circuitry, including the patterning and directional growth of fetal corticofugal axons. In the latter, Saez et al. (2014) show that subcutaneous injection of WIN beginning at gestational day 5, disrupts both radial and tangential migration within the cortex, increasing the number of migrating GABAergic neurons during late gestation, while leaving cortical apoptosis unaffected. Previous studies also revealed an increase in CCK mRNA in the hippocampus following prenatal THC treatment as well as impaired postsynaptic target selection among a subpopulation of vesicular glutamate transporter 3 (Vglut3)-expressing CCK-INTs in mice with conditional CB1R deletion[11, 12].

While these findings contrast with our study, the techniques used lack the specificity to precisely examine the CCK-INT population currently examined. CCK mRNA is promiscuous within the hippocampus and can be found in a variety of interneurons as well as pyramidal cells. In addition, experiments showing an increase in CCK mRNA were performed in rats and at an earlier time point (P6), when CCK-INTs cannot be reliably detected immunocytochemically and INT populations in general are rapidly declining, making it difficult to extrapolate to mature CCK-INT patterning. Analysis of the effects of exogenous cannabinoid exposure on GABAergic INT tangential migration relied on immunostaining for the entire GABAergic INT population and focused on one developmental time point, leaving open the possibility that temporal control of tangential migration may be disrupted. With regard to findings on axonal mistargeting of Vglut3+ CCK-INTs, our study did not examine the effect of prenatal WIN or THC exposure on subpopulations of CCK-INTs focusing instead on the entire cell population. Recent evidence showing morphological differences between Vglut3+ and non-Vglut3+ CCK-INT terminals suggest exogenous cannabinoid exposure may differentially affect the two subpopulations[48]. Further study is required in order to assess whether prenatal WIN or THC treatment has variable effects on distinct CCK-INT subpopulations.

Despite these incongruities, these studies, as well as ours add to a growing base of literature on the role of CB1Rs and eCB signaling in the developing brain. Evidence indicates a role for CB1Rs in neuronal proliferation, specification, migration and axon outgrowth, supporting a model where the dynamic balance of the eCB synthesizing (diacylglycerol lipase [DAGL]) and hydrolyzing (monoacylgylcerol lipase [MAGL]) enzymes governs the role of CB1R signaling in these various phases of development [11–13, 49]. The location of DAGL and MAGL at various phases of development provides spatial and temporal control over eCB signaling, delivering cell-state specific regulation of CB1R activation [50]. As exogenous cannabinoids are insensitive to hydrolysis by MAGL, they can disrupt the spatial organization of eCB signaling, and consequently, disrupt the developmental programs governed by CB1Rs [15, 50]. Though the selective loss of CCK-INTs suggests a cell autonomous mechanism, evidence linking prenatal cannabinoid exposure to disruption of corticofugal and corticospinal axon projections from forebrain glutamatergic principle neurons suggests potential for non-cell autonomous mechanisms as well. Disruption of

distinct principle cell subpopulations may alter the extracellular milieu during development, disrupting chemical gradients necessary for tangential cell migration or cell survival cues, and could precipitate CCK-INT deficits. While our findings did not attempt to identify the specific aspect of CCK-INT development that is disrupted by exogenous cannabinoid application, our anatomical and physiological findings contribute to the nascent body of literature describing cannabinoid-mediated disruption of neuronal development. Further research is needed to elucidate the specific mechanism underlying the deficits in CCK-INT density and function found in our model of prenatal cannabinoid exposure.

Previous studies indicate that pre/perinatal exogenous cannabinoid exposure is associated a variety of neurobehavioral defects [47, 51–53]. Interestingly, in our model we found that prenatal WIN exposure was associated specifically with deficits in social interaction but not anxiety-related behavior. These discrepancies could correspond to differences in the treatment window as well as differences in the animal model. In previous studies that showed anxiogenic behavior, altered social behavior and deficits in learning and memory related tasks, exogenous cannabinoids were applied perinatally from embryonic day 15(E15) to postnatal day 9(P9)[47, 52]. As the role of developmental eCB signaling is age-dependent, both timing and duration of exogenous cannabinoid exposure likely dictates which aspects of eCB dependent neuronal development and maturation are affected, influencing the observed phenotype[54].

Our findings add to the growing body of evidence implicating altered excitation/inhibition balance in a variety of neuropsychiatric disorders, including autism spectrum disorders (ASD), schizophrenia and epilepsy[55–58]. However, the correlation between hippocampal CCK-INT deficits and the observed deficits in social behavior remains unclear. A recent study showed that adolescent CB exposure is associated with alterations in GABAergic tone in prefrontal cortex (PFC), an area implicated in social information processing, suggesting local PFC disruption of CCK-INT number and function could underlie the observed behavioral phenotype[57, 59]. However, promiscuity of the CCK antibody within mouse cortical regions currently precludes analysis of CCK-INT density in the cortex, limiting our ability to assess the effect of prenatal CB exposure on cortical CCK-INT development. Further, while our model shows a specific deficit in hippocampal CCK-INTs, evidence suggests distinct subpopulations of cortical excitatory neurons may be affected by prenatal CB exposure as well. This indicates the observed behavioral phenotype may be precipitated by alterations to both CCK-INTs and specific PC subpopulations[15, 18].

CB1R activation is a critical modulatory mechanism inhibiting transmitter release from CCK-INT synapses in both activity-dependent and constitutive manners[60]. Previous findings show that constitutive CB1R activity can be reduced by chronic treatment with TTX or deafferenting organotypic slice cultures, indicating constitutive CB1R activity may provide a homeostatic mechanism that scales specific CB1R+ synapses[44]. Alterations in constitutive CB1R activity have also been shown in two neuroligin-3 mutants associated with ASD, one of which, neurlogin-3 R541C, displays significant increases in hippocampal E/I ratio[46, 61]. These findings along with those presented in this study suggest that disruption of constitutive CB1R activity may be an important hallmark of E/I imbalance in specific neuronal circuits. As the E/I ratio of a particular circuit increases, tipping the balance

towards excitation, a reduction in tonic eCB signaling can increase inhibition mediated by CCK-INTs in an attempt to restore balance.

Overall this study presents an examination of the effect of prenatal exogenous cannabinoid exposure on a specific CB1R+ cell population. These findings add to a nascent body of evidence on the impact of *in utero* cannabis exposure on fetal development and provide a potential cellular mechanism for the persistent neurobehavioral deficits observed in individuals prenatally exposed to cannabis. While regulatory obstacles have made studies on prenatal cannabis exposure difficult, the increasing prevalence of cannabis consumption, precipitated by changes in the legal and social status of the drug, necessitates further research on embryonic exposure. In addition, the rising THC content of recreational cannabis strains and increasing popularity of potent cannabis-derived products make the need for information on prenatal cannabis exposure more pressing as even moderate exposure could prove deleterious.

Supplementary Material

Refer to Web version on PubMed Central for supplementary material.

Acknowledgments

We thank Dr. George Kunos of NIAAA, NIH for generously providing THC. G.A.V. is in the Brown University-NIH Neuroscience Partnership Program. Work supported by an NICHD intramural award to C.J.M.

References

1. National Survey on Drug Use and Health (U.S.), United States. Substance Abuse and Mental Health Services Administration. Office of Applied Studies. National Survey on Drug Use and Health series. Dept. of Health and Human Services, Substance Abuse and Mental Health Services Administration, Office of Applied Studies; Rockville, MD: 2003. Results from the ... National Survey on Drug Use and Health : national findings; p. v
2. Grotenhermen F. Pharmacokinetics and pharmacodynamics of cannabinoids. Clinical pharmacokinetics. 2003; 42(4):327–360. [PubMed: 12648025]
3. Pijlman FT, Rigter SM, Hoek J, Goldschmidt HM, Niesink RJ. Strong increase in total delta-THC in cannabis preparations sold in Dutch coffee shops. Addict Biol. 2005; 10(2):171–180. [PubMed: 16191670]
4. Mehmedic Z, Chandra S, Slade D, Denham H, Foster S, Patel AS, et al. Potency trends of Delta9-THC and other cannabinoids in confiscated cannabis preparations from 1993 to 2008. Journal of forensic sciences. 2010; 55(5):1209–1217. [PubMed: 20487147]
5. Hayatbakhsh MR, Flenady VJ, Gibbons KS, Kingsbury AM, Hurrion E, Mamun AA, et al. Birth outcomes associated with cannabis use before and during pregnancy. Pediatric research. 2012; 71(2):215–219. [PubMed: 22258135]
6. Goldschmidt L, Day NL, Richardson GA. Effects of prenatal marijuana exposure on child behavior problems at age 10. Neurotoxicol Teratol. 2000; 22(3):325–336. [PubMed: 10840176]
7. Goldschmidt L, Richardson GA, Willford JA, Severtson SG, Day NL. School achievement in 14-year-old youths prenatally exposed to marijuana. Neurotoxicol Teratol. 2012; 34(1):161–167. [PubMed: 21884785]
8. Leech SL, Larkby CA, Day R, Day NL. Predictors and correlates of high levels of depression and anxiety symptoms among children at age 10. Journal of the American Academy of Child and Adolescent Psychiatry. 2006; 45(2):223–230. [PubMed: 16429093]

9. Noland JS, Singer LT, Short EJ, Minnes S, Arendt RE, Kirchner HL, et al. Prenatal drug exposure and selective attention in preschoolers. Neurotoxicol Teratol. 2005; 27(3):429–438. [PubMed: 15939203]
10. Howlett AC. The cannabinoid receptors. Prostaglandins & other lipid mediators. 2002; 68–69:619–631.
11. Berghuis P, Dobszay MB, Wang X, Spano S, Ledda F, Sousa KM, et al. Endocannabinoids regulate interneuron migration and morphogenesis by transactivating the TrkB receptor. Proc Natl Acad Sci U S A. 2005; 102(52):19115–19120. [PubMed: 16357196]
12. Berghuis P, Rajnicek AM, Morozov YM, Ross RA, Mulder J, Urban GM, et al. Hardwiring the brain: endocannabinoids shape neuronal connectivity. Science. 2007; 316(5828):1212–1216. [PubMed: 17525344]
13. Mulder J, Aguado T, Keimpema E, Barabas K, Ballester Rosado CJ, Nguyen L, et al. Endocannabinoid signaling controls pyramidal cell specification and long-range axon patterning. Proc Natl Acad Sci U S A. 2008; 105(25):8760–8765. [PubMed: 18562289]
14. Diaz-Alonso J, Aguado T, Wu CS, Palazuelos J, Hofmann C, Garcez P, et al. The CB(1) cannabinoid receptor drives corticospinal motor neuron differentiation through the Ctip2/Satb2 transcriptional regulation axis. J Neurosci. 2012; 32(47):16651–16665. [PubMed: 23175820]
15. Tortoriello G, Morris CV, Alpar A, Fuzik J, Shirran SL, Calvigioni D, et al. Miswiring the brain: Delta9-tetrahydrocannabinol disrupts cortical development by inducing an SCG10/stathmin-2 degradation pathway. The EMBO journal. 2014; 33(7):668–685. [PubMed: 24469251]
16. Alpar A, Tortoriello G, Calvigioni D, Niphakis MJ, Milenkovic I, Bakker J, et al. Endocannabinoids modulate cortical development by configuring Slit2/Robo1 signalling. Nat Commun. 2014; 5:4421. [PubMed: 25030704]
17. Wu CS, Zhu J, Wager-Miller J, Wang S, O'Leary D, Monory K, et al. Requirement of cannabinoid CB(1) receptors in cortical pyramidal neurons for appropriate development of corticothalamic and thalamocortical projections. Eur J Neurosci. 2010; 32(5):693–706. [PubMed: 21050275]
18. de Salas-Quiroga A, Diaz-Alonso J, Garcia-Rincon D, Remmers F, Vega D, Gomez-Canas M, et al. Prenatal exposure to cannabinoids evokes long-lasting functional alterations by targeting CB1 receptors on developing cortical neurons. Proc Natl Acad Sci U S A. 2015
19. Morozov YM, Freund TF. Post-natal development of type 1 cannabinoid receptor immunoreactivity in the rat hippocampus. Eur J Neurosci. 2003; 18(5):1213–1222. [PubMed: 12956720]
20. Morozov YM, Torii M, Rakic P. Origin, early commitment, migratory routes, and destination of cannabinoid type 1 receptor-containing interneurons. Cereb Cortex. 2009; 19(Suppl 1):i78–89. [PubMed: 19346272]
21. Antypa M, Faux C, Eichele G, Parnavelas JG, Andrews WD. Differential gene expression in migratory streams of cortical interneurons. Eur J Neurosci. 2011; 34(10):1584–1594. [PubMed: 22103416]
22. Saez TM, Aronne MP, Caltana L, Brusco AH. Prenatal exposure to the CB1 and CB2 cannabinoid receptor agonist WIN 55,212-2 alters migration of early-born glutamatergic neurons and GABAergic interneurons in the rat cerebral cortex. Journal of neurochemistry. 2014; 129(4):637–648. [PubMed: 24329778]
23. Morozov YM, Freund TF. Postnatal development and migration of cholecystokinin-immunoreactive interneurons in rat hippocampus. Neuroscience. 2003; 120(4):923–939. [PubMed: 12927199]
24. Nagode DA, Tang AH, Yang K, Alger BE. Optogenetic identification of an intrinsic cholinergically driven inhibitory oscillator sensitive to cannabinoids and opioids in hippocampal CA1. J Physiol. 2014; 592(Pt 1):103–123. [PubMed: 24190932]
25. Sauer JF, Struber M, Bartos M. Impaired fast-spiking interneuron function in a genetic mouse model of depression. eLife. 2015; 4
26. Yang, M.; Silverman, JL.; Crawley, JN. Automated three-chambered social approach task for mice. In: Crawley, Jacqueline N., et al., editors. Current protocols in neuroscience / editorial board. Vol. Chapter 8. 2011. p. 26

27. Mereu G, Fa M, Ferraro L, Cagiano R, Antonelli T, Tattoli M, et al. Prenatal exposure to a cannabinoid agonist produces memory deficits linked to dysfunction in hippocampal long-term potentiation and glutamate release. Proc Natl Acad Sci U S A. 2003; 100(8):4915–4920. [PubMed: 12679519]

28. Mato S, Chevaleyre V, Robbe D, Pazos A, Castillo PE, Manzoni OJ. A single in-vivo exposure to delta 9THC blocks endocannabinoid-mediated synaptic plasticity. Nat Neurosci. 2004; 7(6):585–586. [PubMed: 15146190]

29. Chittajallu R, Craig MT, McFarland A, Yuan X, Gerfen S, Tricoire L, et al. Dual origins of functionally distinct O-LM interneurons revealed by differential 5-HT(3A)R expression. Nat Neurosci. 2013; 16(11):1598–1607. [PubMed: 24097043]

30. Tricoire L, Pelkey KA, Erkkila BE, Jeffries BW, Yuan X, McBain CJ. A blueprint for the spatiotemporal origins of mouse hippocampal interneuron diversity. The Journal of neuroscience : the official journal of the Society for Neuroscience. 2011; 31(30):10948–10970. [PubMed: 21795545]

31. Xu Q, Tam M, Anderson SA. Fate mapping Nkx2. 1-lineage cells in the mouse telencephalon. The Journal of comparative neurology. 2008; 506(1):16–29. [PubMed: 17990269]

32. Lee S, Hjerling-Leffler J, Zagha E, Fishell G, Rudy B. The largest group of superficial neocortical GABAergic interneurons expresses ionotropic serotonin receptors. J Neurosci. 2010; 30(50): 16796–16808. [PubMed: 21159951]

33. Somogyi J, Baude A, Omori Y, Shimizu H, El Mestikawy S, Fukaya M, et al. GABAergic basket cells expressing cholecystokinin contain vesicular glutamate transporter type 3 (VGLUT3) in their synaptic terminals in hippocampus and isocortex of the rat. Eur J Neurosci. 2004; 19(3):552–569. [PubMed: 14984406]

34. Bezaire MJ, Soltesz I. Quantitative assessment of CA1 local circuits: knowledge base for interneuron-pyramidal cell connectivity. Hippocampus. 2013; 23(9):751–785. [PubMed: 23674373]

35. Hill EL, Gallopin T, Ferezou I, Cauli B, Rossier J, Schweitzer P, et al. Functional CB1 receptors are broadly expressed in neocortical GABAergic and glutamatergic neurons. J Neurophysiol. 2007; 97(4):2580–2589. [PubMed: 17267760]

36. Donato F, Rompani SB, Caroni P. Parvalbumin-expressing basket-cell network plasticity induced by experience regulates adult learning. Nature. 2013; 504(7479):272–276. [PubMed: 24336286]

37. Cope DW, Maccaferri G, Marton LF, Roberts JD, Cobden PM, Somogyi P. Cholecystokinin-immunopositive basket and Schaffer collateral-associated interneurones target different domains of pyramidal cells in the CA1 area of the rat hippocampus. Neuroscience. 2002; 109(1):63–80. [PubMed: 11784700]

38. Kawamura Y, Fukaya M, Maejima T, Yoshida T, Miura E, Watanabe M, et al. The CB1 cannabinoid receptor is the major cannabinoid receptor at excitatory presynaptic sites in the hippocampus and cerebellum. J Neurosci. 2006; 26(11):2991–3001. [PubMed: 16540577]

39. Pitler TA, Alger BE. Depolarization-induced suppression of GABAergic inhibition in rat hippocampal pyramidal cells: G protein involvement in a presynaptic mechanism. Neuron. 1994; 13(6):1447–1455. [PubMed: 7993636]

40. Wilson RI, Nicoll RA. Endogenous cannabinoids mediate retrograde signalling at hippocampal synapses. Nature. 2001; 410(6828):588–592. [PubMed: 11279497]

41. Glickfeld LL, Scanziani M. Distinct timing in the activity of cannabinoid-sensitive and cannabinoid-insensitive basket cells. Nature Neuroscience. 2006; 9(6):807–815. [PubMed: 16648849]

42. Basu J, Srinivas KV, Cheung SK, Taniguchi H, Huang ZJ, Siegelbaum SA. A cortico-hippocampal learning rule shapes inhibitory microcircuit activity to enhance hippocampal information flow. Neuron. 2013; 79(6):1208–1221. [PubMed: 24050406]

43. Neu A, Foldy C, Soltesz I. Postsynaptic origin of CB1-dependent tonic inhibition of GABA release at cholecystokinin-positive basket cell to pyramidal cell synapses in the CA1 region of the rat hippocampus. J Physiol. 2007; 578(Pt 1):233–247. [PubMed: 17053036]

44. Kim J, Alger BE. Reduction in endocannabinoid tone is a homeostatic mechanism for specific inhibitory synapses. Nat Neurosci. 2010; 13(5):592–600. [PubMed: 20348918]

45. Hefft S, Jonas P. Asynchronous GABA release generates long-lasting inhibition at a hippocampal interneuron-principal neuron synapse. Nature Neuroscience. 2005; 8(10):1319–1328. [PubMed: 16158066]
46. Foldy C, Malenka RC, Sudhof TC. Autism-associated neuroligin-3 mutations commonly disrupt tonic endocannabinoid signaling. Neuron. 2013; 78(3):498–509. [PubMed: 23583622]
47. Trezza V, Campolongo P, Cassano T, Macheda T, Dipasquale P, Carratu MR, et al. Effects of perinatal exposure to delta-9-tetrahydrocannabinol on the emotional reactivity of the offspring: a longitudinal behavioral study in Wistar rats. Psychopharmacology (Berl). 2008; 198(4):529–537. [PubMed: 18452035]
48. Omiya Y, Uchigashima M, Konno K, Yamasaki M, Miyazaki T, Yoshida T, et al. VGluT3-expressing CCK-positive basket cells construct invaginating synapses enriched with endocannabinoid signaling proteins in particular cortical and cortex-like amygdaloid regions of mouse brains. J Neurosci. 2015; 35(10):4215–4228. [PubMed: 25762668]
49. Aguado T, Palazuelos J, Monory K, Stella N, Cravatt B, Lutz B, et al. The endocannabinoid system promotes astroglial differentiation by acting on neural progenitor cells. The Journal of neuroscience : the official journal of the Society for Neuroscience. 2006; 26(5):1551–1561. [PubMed: 16452678]
50. Keimpema E, Mackie K, Harkany T. Molecular model of cannabis sensitivity in developing neuronal circuits. Trends Pharmacol Sci. 2011; 32(9):551–561. [PubMed: 21757242]
51. Shabani M, Hosseinmardi N, Haghani M, Shaibani V, Janahmadi M. Maternal exposure to the CB1 cannabinoid agonist WIN 55212-2 produces robust changes in motor function and intrinsic electrophysiological properties of cerebellar Purkinje neurons in rat offspring. Neuroscience. 2011; 172:139–152. [PubMed: 20969930]
52. Campolongo P, Trezza V, Cassano T, Gaetani S, Morgese MG, Ubaldi M, et al. Perinatal exposure to delta-9-tetrahydrocannabinol causes enduring cognitive deficits associated with alteration of cortical gene expression and neurotransmission in rats. Addict Biol. 2007; 12(3–4):485–495. [PubMed: 17578508]
53. Spano MS, Ellgren M, Wang X, Hurd YL. Prenatal cannabis exposure increases heroin seeking with allostatic changes in limbic enkephalin systems in adulthood. Biol Psychiatry. 2007; 61(4): 554–563. [PubMed: 16876136]
54. Maccarrone M, Guzman M, Mackie K, Doherty P, Harkany T. Programming of neural cells by (endo)cannabinoids: from physiological rules to emerging therapies. Nat Rev Neurosci. 2014; 15(12):786–801. [PubMed: 25409697]
55. Kehrer C, Maziashvili N, Dugladze T, Gloveli T. Altered Excitatory-Inhibitory Balance in the NMDA-Hypofunction Model of Schizophrenia. Frontiers in molecular neuroscience. 2008; 1:6. [PubMed: 18946539]
56. Calfa G, Li W, Rutherford JM, Pozzo-Miller L. Excitation/Inhibition imbalance and impaired synaptic inhibition in hippocampal area CA3 of Mecp2 knockout mice. Hippocampus. 2014
57. Yizhar O, Fenno LE, Prigge M, Schneider F, Davidson TJ, O'Shea DJ, et al. Neocortical excitation/inhibition balance in information processing and social dysfunction. Nature. 2011; 477(7363):171–178. [PubMed: 21796121]
58. Ziburkus J, Cressman JR, Schiff SJ. Seizures as imbalanced up states: excitatory and inhibitory conductances during seizure-like events. J Neurophysiol. 2013; 109(5):1296–1306. [PubMed: 23221405]
59. Cass DK, Flores-Barrera E, Thomases DR, Vital WF, Caballero A, Tseng KY. CB1 cannabinoid receptor stimulation during adolescence impairs the maturation of GABA function in the adult rat prefrontal cortex. Molecular psychiatry. 2014; 19(5):536–543. [PubMed: 24589887]
60. Lee SH, Soltesz I. Requirement for CB1 but not GABAB receptors in the cholecystokinin mediated inhibition of GABA release from cholecystokinin expressing basket cells. J Physiol. 2011; 589(Pt 4):891–902. [PubMed: 21173082]
61. Etherton M, Foldy C, Sharma M, Tabuchi K, Liu X, Shamloo M, et al. Autism-linked neuroligin-3 R451C mutation differentially alters hippocampal and cortical synaptic function. Proc Natl Acad Sci U S A. 2011; 108(33):13764–13769. [PubMed: 21808020]

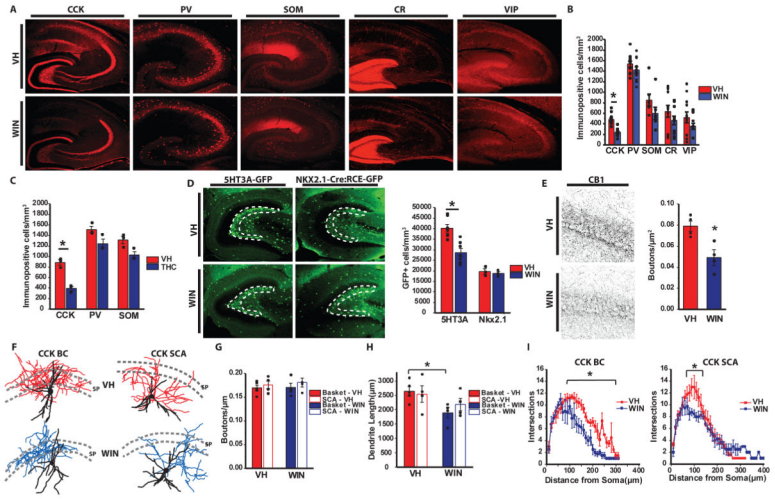

Figure 1. Loss of CCK-INTs following in utero THC or WIN exposure

A) Representative images of CCK, PV, SOM, CR and VIP labeling in hippocampal sections from mice born to VH or WIN treated mothers. **B)** Summary plot of the density of labeled cells for each marker in paired VH/WIN treated litters. 11 mice from 11 litters/treatment were examined for CCK and PV, 10 mice from 10 litters/treatment for SOM, and 12 mice from 12 litters/treatment for CR and VIP (*$p=5\times10^{-6}$). **C)** Summary plot of the density of labeled cells for CCK, PV and SOM in paired VH/THC treated litters. Three mice from three litters/treatment were examined for each marker (*p=0.001). **D)** Representative images (left) and summary plot (right) of GFP+ cell labeling in *5HT3AR-GFP* and *Nkx2.1-Cre:RCE-GFP* mice born to VH or WIN treated mothers. Dashed lines indicate the region of interest for cell counts. For *5HT3AR-GFP* 7 mice from seven WIN or VH treated litters were examined (*$p=3.9\times10^{-9}$) and for *Nkx2.1-Cre:RCE-GFP* mice 3 mice from 3 litters/treatment were analyzed. **E)** Representative images (left) and group data counts (right) for CCK-INT bouton stains with CB1R after prenatal treatment with VH or WIN. 4 mice from 4 litters/treatment were counted (*p=0.02). **F)** Drawings of reconstructed CCK-BCs (left) and SCAs (right) recorded VH (top) and WIN (bottom) treated animals. Dendrites are black for both treatment groups while axons are colored red and blue for VH and WIN treated animals, respectively. Dashed lines indicate the borders of SP. **G)** Quantification of terminal density along the axon of CCK-BCs and SCAs in VH and WIN treated animals (CCK-BCs: VH: n=5, WIN=4; SCAs: n=4/treatment). **H)** Quantification of total dendrite length for CCK-BS and SCAs in VH and WIN treated animals (*p=0.03). **I)** Sholl analyses for dendrites of CCK-BCs (left) and SCAs (right) in VH or WIN treated mice (*p=0.03, for both). Values are plotted as mean±SEM.

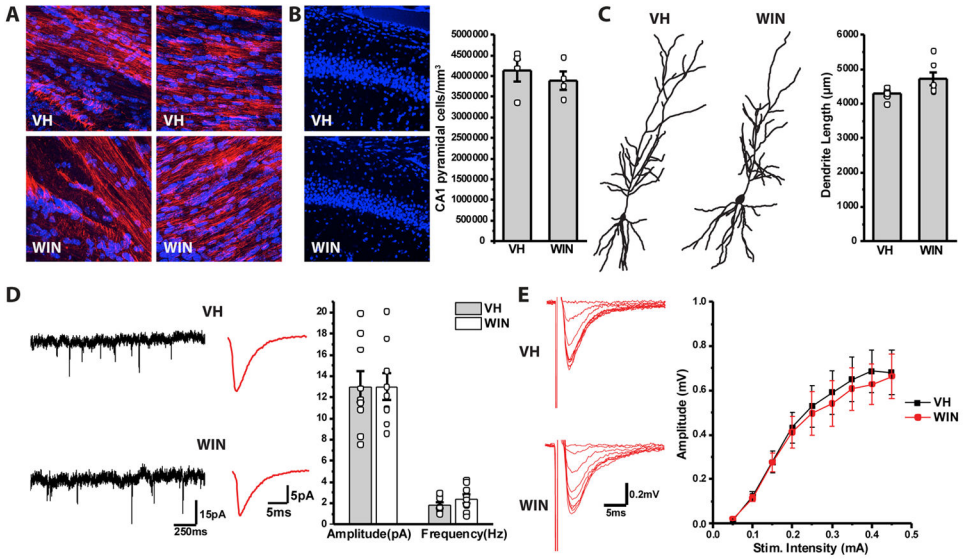

Figure 2. WIN exposure does not affect PC morphology or physiology

A) Images of L1NCAM (red) and Hoechst (blue) staining in both VH (*top*) and WIN (*bottom*) treated animals. Images show normal patterning of projections in both the corpus collosum (*left*) and fimbria (*right*). **B)** Left panel shows sample images of Hoechst stain in CA1 of VH (*top*) and WIN (*bottom*) treated animals. Right panel shows summarized data of PC density in CA1 of VH and WIN treated animals (VH: n=4 mice/4 litters, WIN: n=4 mice/4 litters). **C)** Left panel shows drawings of reconstructed PCs in VH (*left*) and WIN (*right*) treated mice. Right panel shows summarized plot of PC dendritic length in VH and WIN treated animals (VH: n=6 cells/3 mice/2 litters, WIN: n=6 cells/3 mice/2 litters). **D)** Continuous traces (*left*) and representative waveform (*middle*) of sEPSCs recorded in CA1 PCs of VH (*top*) and WIN (*bottom*) treated mice. Right panel shows summarized data for sEPSC amplitude and frequency in VH and WIN mice (VH: n=9 cells/2 mice/2 litters, WIN: n=9 mice/2 mice/2 litters). **E)** Left panel shows representative traces of field EPSPs recorded in CA1 stratum radiatum of VH (*top*) and WIN (*bottom*) animals following stimulation of the Schaffer collateral pathway at increasing intensity. Left panel shows summarized plot of input/out dynamics in VH and WIN mice depicting field EPSP amplitude at various stimulation intensities (VH: n=9 slices/3 mice/2 litters, WIN: n=9 slices/3 mice/2 litters).

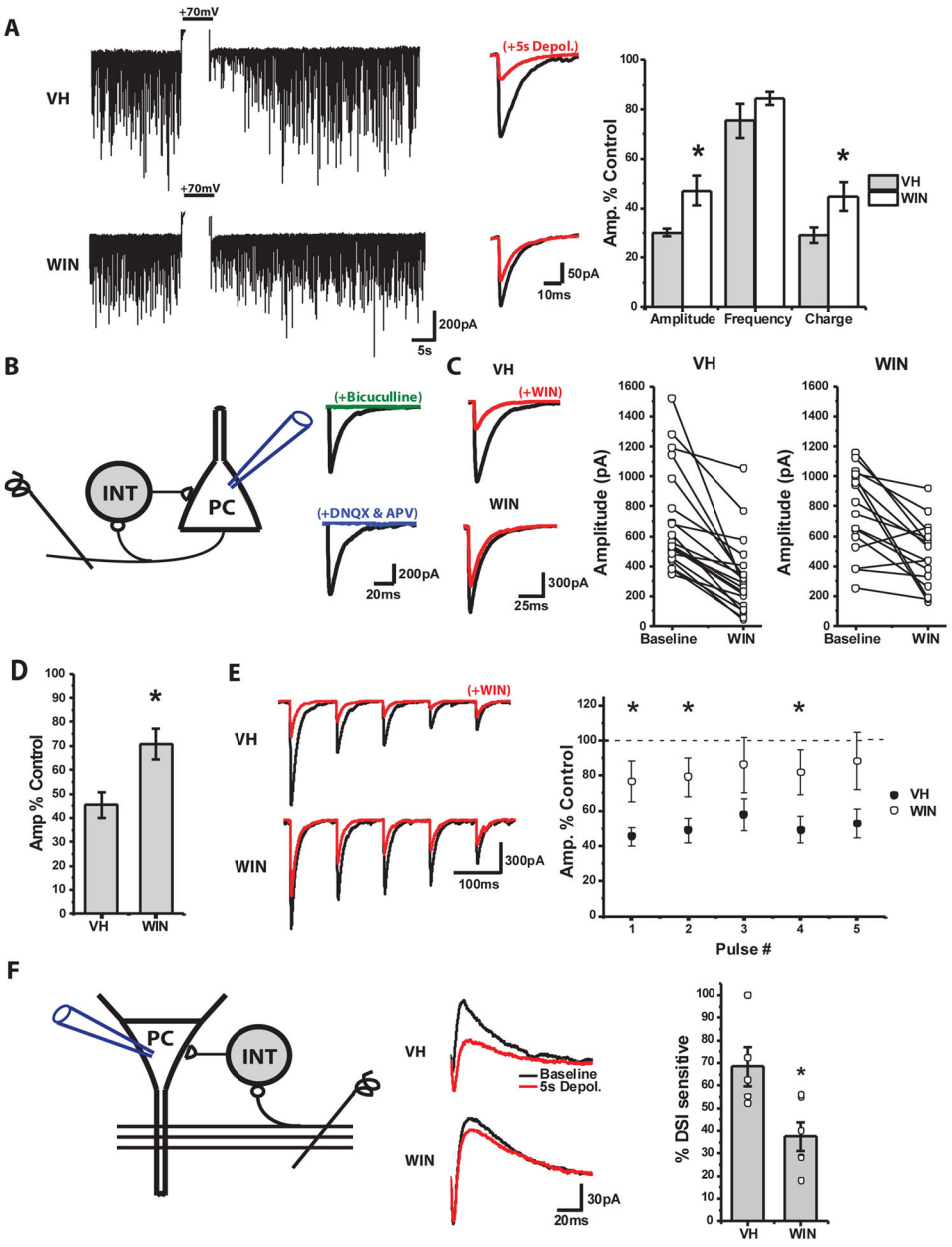

Figure 3. Deficient CCK-INT mediated inhibitory drive in prenatally WIN treated mice

A) At left are continuous traces of representative CA1 PC recordings showing sIPSCs before and after DSI induction (+70mV, truncated) in VH or WIN treated mice. Middle panel shows averaged sIPSC waveforms for events obtained for 5s before and after DSI induction. Group data plotted at right highlights changes in amplitude, frequency and charge of sIPSCs following DSI induction expressed as percentage of pre-DSI levels (VH: n=8 cells/3 animals/2 litters, WIN: n=11 cells/3 animals/2 litters; *Amplitude p=0.03, *Charge: p=0.03. **B)** Schematic of feedback inhibition evoked by alvear stimulation (left) and averaged CA1 IPSCS (right) from representative recordings illustrating sensitivity to both GABA (Bicuculline, 10μM) and glutamate (DNQX, 10μM/dl-AP5, 50μM) antagonism confirming their disynaptic nature. **C)** At left are averaged disynaptically evoked IPSC waveforms from

representative recordings before and after acute WIN (1μM) application in VH and WIN treated mice. Group data plots to the right show acute WIN effects on IPSC amplitudes for each recording. **D)** Summarized data shown as % of control amplitudes obtained prior to acute WIN application (right; VH: n=20 cells/11 animals/5 litters, WIN: n=16 cells/10 animals/6 litters; * p=0.01). **E)** Representative example traces (left) and group data summary (right) illustrating the effect of acute WIN application on 5 pulse trains of disynaptically evoked IPSCs in VH and WIN treated mice (VH: n=20 cells/11 animals/5 litters, WIN: n=16 cells/10 animals/6 litters; p=0.01, 0.02, 0.10, 0.03, and 0.05 for pulses 1–5 respectively). **F)** Schematic of feedforward inhibition evoked by Schaffer collateral stimulation (left). At middle are averaged feedforward evoked waveforms showing the inward monosynaptic excitatory current and outward disynaptic inhibitory current. Right panel shows summarized plot of the % of disynaptic inhibition that is sensitive to DSI in both VH and WIN treated mice (VH: n=5 cells/3 animals/2 litters, WIN: n=6 cells/3 animals/3 litters; p=0.03).

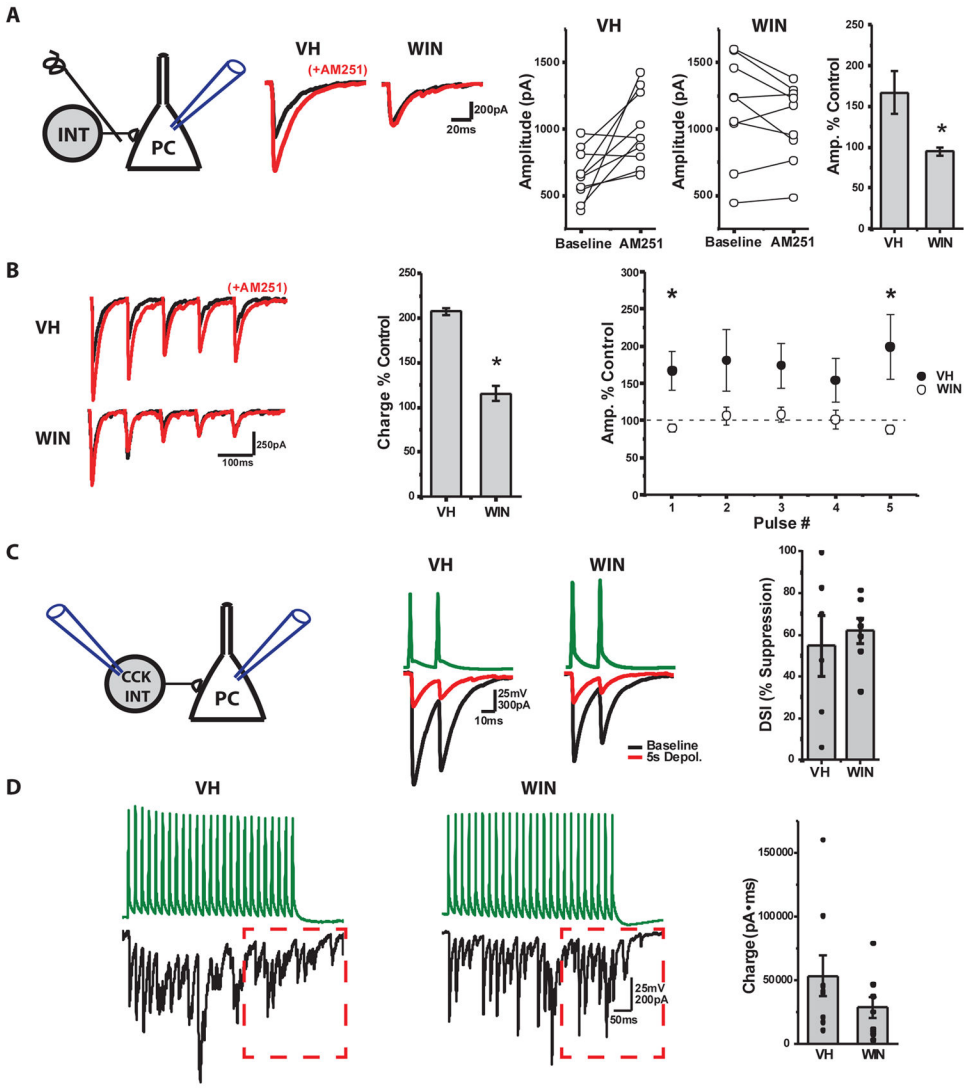

Figure 4. Loss of tonic eCB mediated inhibition of CCK-BC release in WIN treated mice

A) Schematic diagram (*left*), averaged IPSC traces from representative recordings (*middle*), and group data summary plots (*right*) illustrating the effects of the CB1R antagonist AM251 (10 μM) on basal CCK-BC to CA1 PC transmission in VH and WIN treated mice (VH: n=10 cells/4 animals/1 litter, WIN: n=9 cells/3 animals/2 litters; * p=0.01). **B)** Effect of AM251 on trains of monosynaptically evoked CCK-BC to PC IPSCs in VH and WIN treated mice. Shown are averaged IPSC trains from representative recordings (left) and group data summaries for changes in total charge during the train (middle, *p=0.03) or amplitudes of each event during the trains (right, p=0.01, 0.11, 0.06, 0.13, and 0.03 for pulses 1–5 respectively) expressed as %s of control responses obtained before AM251 (VH: n=10 cells/4 animals/1 litters, WIN: n=9 cells/3 animals/2 litters,). **C)** Schematic diagram of CCK-INT to PC paired recording (*left*), representative traces of unitary events before and after DSI induction (*middle*) and group data summary of DSI amplitude changes expressed as % inhibition of pre-DSI levels (*right*) for connected pairs in VH and WIN treated mice (VH: n=6 pairs/4 animals/2 litters), WIN: n=6 pairs/4 animals/2 litters). **D)** Single trial

traces from representative CCK-INT to PC pairs (*left*) and group data summary (*right*) illustrating the degree of asynchronous release from CCK-INTs during train activity in VH and WIN treated mice. Asynchronicity was measured as the charge transfer during a 300ms window centered on the peak of the last AP in the train (boxed region; VH: n=9 pairs/6 animals/2 litters, WIN: n=8 pairs/6 animals/2 litters).

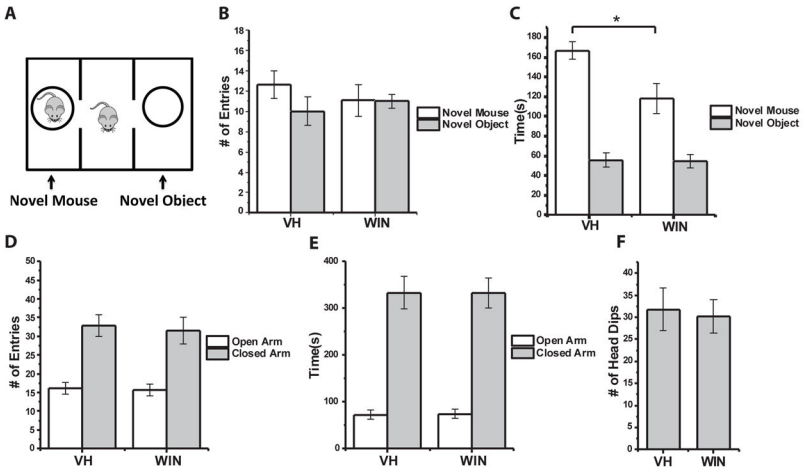

Figure 5. Reduced social interaction in WIN treated mice

A) Schematic diagram of three-chamber social interaction test. **B)** Group data summarizing the number entries mice from each treatment group made into chambers containing the novel mouse or object. **C)** Group data showing the total time mice from each treatment group spent interacting with the novel mouse and novel object (*p=0.01). **D–E)** Elevated plus maze group data summarizing the number of entries (D) and total time spent (E) in the open and closed arms of the maze for VH and WIN treated mice. **F)** Summary of the number of head dips mice from each treatment made during elevated plus maze testing. 11 mice from 3 litters were evaluated per treatment group for each behavioral test.